



ISSN: 2723-9535

Available online at [www.HighTechJournal.org](http://www.HighTechJournal.org)

# HighTech and Innovation Journal

Vol. 4, No. 3, September, 2023



## Comprehensive Evaluation of Deep Neural Network Architectures for Parawood Pith Estimation

Wattanapong Kurdthongmee<sup>1\*</sup> 

<sup>1</sup> School of Engineering and Technology, Walailak University 222 Thaiburi, Thasala, Nakhon Si Thammarat 80160, Thailand.

Received 04 June 2023; Revised 05 August 2023; Accepted 17 August 2023; Published 01 September 2023

### Abstract

Accurate pith estimation is crucial for maintaining the quality of wood products. This study delves into deep learning techniques for precise Parawood pith estimation, employing popular convolutional neural networks (ResNet50, MobileNet, and Xception) with adapted regression heads. Through variations in regression functions, optimizers, and training epochs, the most effective models were pinpointed. Xception, coupled with Huber Loss regression, Nadam optimizer, and 200 epochs, showcased superior performance, achieving a 4.48 mm mean error (with a standard deviation of 3.69 mm) in Parawood. Notably, benchmarking on the Douglas Fir dataset yielded similar results (2.81 mm mean error, standard deviation: 1.57 mm). These findings underscore deep learning's potential for Parawood and Douglas Fir pith estimation, offering substantial benefits to wood industry quality control and production efficiency. By harnessing advanced machine learning techniques, this study advances wood industry processes, promoting the adoption of state-of-the-art technology in forestry and wood science.

**Keywords:** Wood Pith Detection; Parawood; Deep Learning; Resnet; Mobilenet; Xception; Image Augmentation; Regression; Accuracy.

## 1. Introduction

Accurate estimation of the pith, the central core of a tree, is pivotal in the fields of wood science and forestry. It profoundly influences the quality and value of wood products [1, 2], impacting their strength, durability, and overall appeal. Over recent years, the pursuit of automated methods for precise pith estimation has gained momentum, leveraging advanced imaging and machine learning techniques. These methods hold great promise for enhancing the efficiency and accuracy of pith estimation, offering valuable insights for wood quality assessment and grading [3].

Despite these advances, there is a critical scientific gap. While some progress has been made in pith estimation techniques, challenges remain. Existing methods, whether based on annual ring relationships, local orientation estimation, or deep neural networks (DNN) [4], have limitations that hinder the attainment of truly accurate and efficient pith estimation. This paper seeks to bridge this gap by presenting a novel approach that addresses these limitations and pioneers a new era in pith estimation. The significance of precise pith estimation extends beyond the realm of research, resonating deeply with the wood industry. Take, for instance, the case of parawood, a prized hardwood employed extensively in furniture production. While parawood's high density and hardness make it an attractive material, its large central pith can jeopardize the quality and strength of finished products. Therefore, meticulous pith estimation in parawood is paramount to optimizing its use in furniture manufacturing. Recent advancements using X-ray computed tomography (CT) imaging underscore the importance of accurate pith estimation in enhancing wood utilization and the quality of end products [5, 6].

\* Corresponding author: [kwattana@wu.ac.th](mailto:kwattana@wu.ac.th)

 <http://dx.doi.org/10.28991/HIJ-2023-04-03-06>

➤ This is an open access article under the CC-BY license (<https://creativecommons.org/licenses/by/4.0/>).

© Authors retain all copyrights.

A thorough exploration of the state of the art reveals a landscape where traditional methods, such as annual ring analysis [7–12] and local orientation estimation [13–15], while effective to a degree, necessitate substantial preprocessing and manual labor. Recent forays into automated pith detection using DNN object detection algorithms, like YOLO [16] and SSD MobileNet [17], have shown promise but leave room for improvement. The question of how to achieve accurate and efficient pith estimation in an automated and accessible manner remains unanswered.

Recently, automated pith detection in wood using DNN (Deep Neural Networks) object detection algorithms has gained attention, with YOLO (You-Only-Look-Once) object detection being proposed for wood pith identification [16]. In one study, the Tiny-YOLO network was trained using transfer learning on 345 wood cross-sectional images, achieving a detection rate of 76.3% and an average distance error of 16.6 pixels [16]. In another study, Kurdthongmee et al. compared the effectiveness of two DNN algorithms, SSD (Single-Shot Detector) MobileNet and YOLO, for detecting pith in Parawood. SSD MobileNet achieved the best detection rate of 87.7%, making it an effective approach for automating Parawood pith detection in cross-sectional images [17]. Furthermore, Kurdthongmee et al. proposed a framework to create a deep learning-based object detector with a limited dataset by training the detector with the regions surrounding an object. The proposed algorithm post-processes the detection results to identify the object. This framework was applied to the problem of wood pith approximation using the YOLO v3 framework and a wood pith dataset with only 150 images. Experiments were conducted to compare the detection results from different approaches to preparing the regions surrounding a pith. The best experiment result shows that the framework outperforms the typical approach with approximately twice the detection precision at a relative average error [18].

The existing literature highlights significant progress in automated wood pith detection using Deep Neural Networks (DNN) object detection algorithms, particularly with the adoption of YOLO (You-Only-Look-Once) object detection [16]. Notably, these studies have achieved commendable detection rates and accuracy in pith identification [16, 17]. However, there are notable gaps in the current literature.

Firstly, while these studies showcase the potential of DNN-based approaches, they predominantly focus on detection and object approximation, leaving room for improved precision in pith estimation. The specific challenge of precisely determining the size and location of the pith within wood, especially in hardwood species like Parawood, remains under addressed. This gap indicates the need for a novel approach that not only detects pith but also provides accurate estimations of its dimensions.

Secondly, the literature, including the recent study by Kurdthongmee et al. [18], has demonstrated that limited-sized datasets can hinder the effectiveness of DNN-based wood pith detection. The need for extensive data and resources in training DNN models is evident, and current solutions such as post-processing and region preparation have room for improvement. Therefore, there is a gap in developing more efficient and accurate methods for pith detection, especially in situations where dataset sizes are constrained.

To address these gaps, our approach innovatively modifies popular deep neural networks, such as ResNet, MobileNet, and Xception, to perform regression tasks instead of classification. By tailoring these networks to estimate the precise location and size of the pith, we aim to significantly enhance the quality and reliability of pith estimation in wood, effectively filling the existing gap in the literature. Furthermore, our research explores the efficiency of model creation by identifying less effective optimization techniques and regression functions, providing insights to guide future research in the wood industry and ultimately contributing to more effective and efficient pith estimation methodologies.

In this paper, we propose a novel approach for Parawood pith estimation by modifying popular deep neural networks, such as ResNet, MobileNet, and Xception, to perform regression instead of classification. Our approach demonstrates several contributions:

- **Improved estimation accuracy:** By adapting the heads of deep neural networks for regression tasks, we achieve more accurate and precise pith estimation results compared to traditional classification-based approaches. This enhances the overall quality and reliability of pith estimation in Parawood.
- **Efficiency in model creation:** Through our experiments, we provide preliminary evidence supporting the future application of modified deep neural networks for regression tasks. Our findings suggest that certain optimizers and regression functions, such as Stochastic Gradient Descent, Log Cosh, Mean Squared Logarithmic Error, and Cosine Similarity, are less effective for pith estimation. This insight can guide researchers and practitioners toward more promising optimization techniques and regression functions for similar regression-based tasks in the wood industry.
- **A platform for future research:** Our work serves as a platform for further investigation and exploration of modified deep neural networks for pith estimation and related applications in the wood products industry. The demonstrated improvements in accuracy and efficiency lay the foundation for future advancements in pith estimation techniques, contributing to enhanced wood product manufacturing processes and cost reduction.

Overall, our approach provides valuable insights into the potential benefits of modifying popular deep neural networks for regression tasks. It offers a preliminary result that supports future research in optimizing the model creation process for pith estimation. By harnessing the strengths of deep neural networks and avoiding less effective optimization and regression techniques, we pave the way for more effective and efficient pith estimation methodologies in the wood industry. The organization of this paper is as follows: the materials and methods are detailed in Section 2. The experiment results and discussions are then provided in Section 3. Finally, the paper is concluded in Section 4.

## 2. Materials and Methods

This section describes the experimental setup and procedures employed in this study to investigate and evaluate the effectiveness of our proposed approach for pith estimation in wood cross-sectional images. We outline the dataset used, consisting of cross-sectional images of Parawood obtained from sawmills in southern Thailand and European origin samples. The specific steps involved in preprocessing the images, including resizing and normalization, are detailed. We then provide an overview of the deep learning models utilized, namely ResNet50, MobileNet, and Xception, as well as the modifications made to their architecture for regression-based pith estimation. The training process, including the selection of optimizers, regression functions, and training epochs, is explained. Additionally, we describe the evaluation metrics employed to assess the performance of the models. The details provided in this section form the foundation for the subsequent analysis and results presented in this study.

### 2.1. Dataset

#### 2.1.1. Training and Testing Dataset

In this study, our objective was to create a dataset of Parawood cross-sectional images that accurately represents the variability of real-world working environments within sawmills in southern Thailand. To achieve this, we utilized a smartphone camera to capture images of the entire cross-sectional area of Parawood logs under natural lighting conditions. The resulting images were saved in JPG format with a size of 4,896×3,264 pixels.

Our dataset comprises a total of 290 images, which can be obtained upon request. By using a smartphone camera to capture the images, we ensured that the dataset accurately reflects the conditions of real-world working environments within sawmills in southern Thailand. This comprehensive dataset will be useful for future research in the field of Parawood cross-sectional image analysis and pith estimation.

Parawood is a by-product of non-economical latex-producing trees, and its surface can often contain various imperfections such as diffused latex, moulds, and defects resulting from the cutting process, as demonstrated in Figure 1. These imperfections can hinder the visibility of the pith, making it difficult for computer vision methods to accurately detect and estimate its location. As a result, significant pre-processing efforts, such as mechanical or chemical methods, are often required to remove these imperfections and enhance the visibility of the pith. However, these pre-processing stages can be labour-intensive and time-consuming, leading to higher production costs and longer processing times. Therefore, it is essential to develop accurate and efficient methods for pith estimation that can handle these imperfections without the need for extensive pre-processing. This will improve the efficiency and sustainability of the Parawood industry.



**Figure 1. Examples of Parawood cross-sectional images from both the training and testing datasets, showing various disturbances such as mold, diffused latex, and rough surfaces resulting from low-quality sawing**

To increase the variability of the dataset and account for potential differences in lighting and other environmental conditions, we applied image augmentation techniques to the original images. This involved modifying the images by:

- Adjusting brightness by up to 25%;
- Blurring by up to 2.5 pixels, and;
- Adding noise to up to 5% of the pixels.

Brightness, blur, and noise were used because they can mimic real-world variability and enhance the diversity of the training dataset.

Adjusting brightness can simulate different lighting conditions, such as shadows or reflections, which may be present in real-world images. This can help the model learn to recognize objects and features under different lighting conditions, leading to more robust performance. Blurring can simulate different levels of focus or depth of field, which can occur in real-world images due to camera settings or distance from the subject. This can help the model learn to recognize objects and features that may be partially obscured or out of focus.

Adding noise can simulate various types of imperfections or artifacts that may be present in real-world images, such as dust, scratches, or compression artifacts. This can help the model learn to recognize objects and features in noisy or low-quality images, leading to more robust performance in real-world scenarios. By applying these image augmentation techniques, the model can learn to be more resilient to variations and imperfections in the input images, leading to better performance on new and unseen data. The use of image augmentation techniques allowed us to generate a larger dataset of 2,900 images for both the training and testing datasets, which was more representative of real-world scenarios and contributed to the robustness of our model.

To facilitate the annotation process, the images within the dataset were previously annotated to indicate the area surrounding the pith. In our experiment, the ground truth pith location was defined as the center of the annotated bounding box. Overall, the comprehensive and variable dataset we have created will aid in the development of more accurate and robust models for Parawood pith estimation. The whole dataset is downloadable from: <https://app.roboflow.com/wattanapong-kurdthongmee/parawoodpithsonde/3>.

### 2.1.2. Validation Dataset

In order to further evaluate the effectiveness and generalizability of our proposed approach, we utilized two additional datasets for validation and benchmarking.

The first dataset, consisting of 900 Parawood pith cross-sectional images, was used for validation purposes. These images were captured under real-world working environments in sawmills, ensuring that they were representative of the conditions encountered in the Parawood industry. This blind dataset was used to evaluate the accuracy and robustness of our model on previously unseen data. The dataset is available upon request to the research community, enabling others to reproduce our results and build upon our work.

The second dataset, consisting of 65 images of European origin wood, was used for benchmarking. This dataset allowed us to compare the performance of our model against existing methods on a different type of wood, enabling us to assess the generalizability of our approach.

## 2.2. Methods

### 2.2.1. Backbones

In our study, ResNet50, MobileNet, and Xception were chosen as the convolutional neural network (CNN) architectures for training and validation. We selected these models based on their effectiveness in feature extraction and processing in image classification tasks.

ResNet50 [19] is a deep CNN architecture that introduced the concept of residual learning, with 50 convolutional layers and residual blocks composed of convolutional layers and skip connections. MobileNet [20], on the other hand, is a lightweight CNN architecture designed for mobile and embedded devices. It is based on depthwise separable convolutions, which decompose standard convolutions into depthwise and pointwise convolutions, reducing computational cost and memory requirements while maintaining high accuracy. The MobileNet family includes MobileNetV1, MobileNetV2, and MobileNetV3, with each version improving accuracy and efficiency.

Xception [21] is another CNN architecture based on the Inception architecture that uses depthwise separable convolutions to replace standard convolutions in Inception. This modification makes Xception more efficient and accurate. The network comprises depthwise separable convolutional layers, global average pooling, and fully connected layers.

To evaluate the effectiveness and generalizability of our approach, we utilized ResNet50, MobileNet, and Xception for training and validation. These CNN architectures have been widely recognized and utilized for their effectiveness in image classification tasks.

### 2.2.2. Heads and Model Variations

In our study, we modified the ResNet50, MobileNet, and Xception architectures by removing their classification heads and replacing them with regression heads. This was done to enable us to accurately estimate the location of the pith in Parawood.

To accomplish this, we utilized a variety of regression functions, the equations of which are listed in Table 1, as follows:

- Mean Square Error (MSE): MSE is a common regression loss function that computes the average squared difference between the predicted and actual values. It penalizes larger errors more heavily than smaller errors and is commonly used in neural network regression tasks.
- Mean Absolute Error (MAE): MAE is another common regression loss function that computes the average absolute difference between the predicted and actual values. It is less sensitive to outliers than MSE and is often used when the target variable has a high variance.
- Log-cosh: Log-cosh is a smooth approximation of the mean absolute error (MAE) that is less sensitive to outliers than MSE. It is defined as the logarithm of the hyperbolic cosine of the difference between the predicted and actual values.
- Huber Loss: Huber Loss is a loss function that is less sensitive to outliers than MSE and MAE. It uses a delta parameter to differentiate between smaller and larger errors and applies MAE to smaller errors and MSE to larger errors.
- Mean Absolute Percentage Error (MAPE): MAPE is a common regression loss function that computes the average absolute percentage difference between the predicted and actual values. It is often used in forecasting tasks when the target variable has a non-zero mean.
- Mean Squared Logarithmic Error (MSLE): MSLE is a loss function that penalizes underestimates more heavily than overestimates. It is commonly used in tasks where the target variable has a large dynamic range.
- Cosine Similarity: Cosine similarity is a measure of similarity between two vectors that is widely used in machine learning. It measures the cosine of the angle between two vectors, with values ranging from -1 (completely dissimilar) to 1 (identical). In the context of regression, cosine similarity can be used as a loss function to encourage the predicted and actual values to be more similar.

**Table 1. Regression functions used in the study**

Regression Function	Equation
Mean Squared Error (MSE)	$\frac{1}{n} \sum_{i=1}^n (y_i - \hat{y}_i)^2$
Mean Absolute Error (MAE)	$\frac{1}{n} \sum_{i=1}^n  y_i - \hat{y}_i $
Log Cosh	$\log(\cosh(\hat{y}_i - y_i))$
Huber Loss	$\begin{cases} \frac{1}{2}(y_i - \hat{y}_i)^2, & \text{for }  y_i - \hat{y}_i  \leq \delta \\ \delta( y_i - \hat{y}_i ) - \frac{1}{2}\delta, & \text{otherwise} \end{cases}$
Mean Absolute Percentage Error (MAPE)	$\frac{1}{n} \sum_{i=1}^n \left  \frac{y_i - \hat{y}_i}{y_i} \right  \times 100\%$
Mean Squared Logarithmic Error (MSLE)	$\frac{1}{n} \sum_{i=1}^n (\log(y_i + 1) - \log(\hat{y}_i + 1))^2$
Cosine Similarity	$1 - \frac{\frac{1}{n} \sum_{i=1}^n y_i \hat{y}_i}{\sqrt{\frac{1}{n} \sum_{i=1}^n y_i^2} \sqrt{\frac{1}{n} \sum_{i=1}^n \hat{y}_i^2}}$

These different regression functions were used in the study to compare their effectiveness in predicting the pith location in Parawood cross-sectional images. In addition to varying the regression functions, we also varied the optimizers used in the training process. This included:

- Adam (Adaptive Moment Estimation): Adam is a popular optimization algorithm that combines the benefits of two other optimization algorithms, Adagrad and RMSprop. It calculates an adaptive learning rate for each parameter by computing exponential moving averages of the gradient and the squared gradient. Adam is efficient and works well in practice, making it a popular choice for many applications.

- **Adagrad (Adaptive Gradient Algorithm):** Adagrad is an optimization algorithm that adapts the learning rate of each parameter based on the historical gradient information. It is particularly useful for sparse data and non-convex optimization problems but can struggle with high-dimensional data.
- **Adadelat:** Adadelat is a variant of Adagrad that addresses some of its limitations. Instead of accumulating all the past gradients, Adadelat keeps a running average of the past gradients and updates the learning rate accordingly. It is well-suited for large datasets and works well for deep learning models with many parameters.
- **Nadam (Nesterov-accelerated Adaptive Moment Estimation):** Nadam is a variant of Adam that incorporates the Nesterov accelerated gradient (NAG) method. NAG helps the algorithm to converge faster by using the gradient at a future point in the optimization process to update the current parameters. Nadam is useful for deep learning models with many parameters and noisy data.
- **Adamax:** Adamax is a variant of Adam that uses the infinity norm to normalize the gradient instead of the L2 norm. This makes it less sensitive to the scale of the gradients and more suitable for optimization problems with very large or very small gradients.
- **RMSprop (Root Mean Square Propagation):** RMSprop is an optimization algorithm that uses a moving average of the squared gradient to adapt the learning rate for each parameter. It helps to prevent the learning rate from becoming too small or too large and is particularly useful for deep learning models with long training times.
- **SGD (Stochastic Gradient Descent):** SGD is a simple optimization algorithm that updates the parameters based on the negative gradient of the loss function. It is computationally efficient and works well for large datasets but can be sensitive to the choice of learning rate and may require more training time to converge compared to other optimization algorithms.

By testing a range of optimizers, we aimed to identify which optimizer would produce the most accurate and efficient results for our model.

Finally, we varied the number of training epochs between 100, 150, 200, and 250. This was done to determine the optimal number of training epochs needed to achieve the most accurate pith estimation. By testing and varying these parameters, we aimed to identify the most effective combination of regression functions, optimizers, and training epochs for pith estimation in Parawood. Ultimately, our goal was to develop a model that could accurately estimate the location of the pith in Parawood logs, thereby contributing to the development of more efficient and sustainable practices within the Parawood industry.

In our study, transfer learning was employed to train all the models. This approach leverages pre-trained weights from a CNN model that has been previously trained on a large dataset like ImageNet. By utilizing these pre-trained weights, the models can benefit from the learned features, resulting in improved accuracy and reduced training time.

For the initialization of our models, we utilized the widely adopted ImageNet weights as a starting point for transfer learning in image classification tasks. These weights were specifically employed to initialize the convolutional layers, which play a crucial role in feature extraction. By leveraging the knowledge captured by the pre-trained weights, our models were able to effectively extract meaningful features relevant to pith estimation.

To train and validate our models, we utilized the Google Colab platform, which provides a GPU-accelerated environment for deep learning tasks. The use of GPU acceleration significantly reduced the training time required for our models and allowed us to run more experiments with different configurations. By employing these techniques, we were able to develop accurate and efficient models for the Parawood pith estimator.

### 2.2.3. Model Quality Metric

To justify the effectiveness of the pith estimation models, the Euclidean distance between the estimated coordinate and the ground truth was used to compute the error. The Euclidean distance is calculated as:

$$d = \sqrt{(x_{pred} - x_{gt})^2 + (y_{pred} - y_{gt})^2} \quad (1)$$

where  $x_{pred}$  and  $y_{pred}$  represent the estimated coordinates of the pith and  $x_{gt}$  and  $y_{gt}$  represent the ground truth coordinates of the pith. This error was computed for each image in the validation dataset, and the resulting metrics were used to determine the final effectiveness of the model.

The metrics used to evaluate the errors included the mean, standard deviation (SD), minimum, and maximum error. The average error represents the average distance between the estimated coordinate and the ground truth across all images in the validation dataset. The standard deviation provides a measure of the spread of the errors around the mean. The minimum and maximum errors represent the smallest and largest errors, respectively, observed in the validation dataset.

By employing these metrics, we discerned the models that exhibited the highest effectiveness in estimating the pith location within Parawood cross-sectional images. Models characterized by lower mean errors and reduced standard deviations were deemed more effective. Such models demonstrated the capacity to estimate the pith location with enhanced accuracy and consistency across various images. Furthermore, models with smaller minimum and maximum errors were regarded as more robust, as they could provide accurate estimations even when faced with challenging or atypical image conditions.

### 3. Results and Discussion

In this experiment, our focus was on developing an effective approach for pith estimation in wood cross-sectional images. We utilized popular deep neural network architectures, namely ResNet50, MobileNet, and Xception, as the backbone models for feature extraction. These models were chosen for their proven capabilities in image classification tasks, making them suitable for our pith estimation objective. Transfer learning was employed, initializing the models with pre-trained weights from ImageNet, to leverage their learned representations.

To enhance the performance of the models, we conducted experiments using different optimization algorithms, including Adam, Adagrad, Adadelta, Nadam, Adamax, RMSprop, and SGD. By examining various optimizers, our objective was to identify the most effective choice for pith estimation. Additionally, we explored a range of regression functions, such as MSE, MAE, Log Cosh, Huber Loss, MAPE, MSLE, and Cosine Similarity. The complete names of these regression functions are provided in Table 1. Through this exploration, we aimed to train the models to accurately estimate the location of the pith.

To investigate the impact of training duration on model performance, we trained the models using varying numbers of epochs, specifically 100, 150, 200, and 250. This allowed us to assess how the duration of training influenced the models' ability to estimate the pith location accurately. The evaluation metrics used to gauge the performance of the models include mean, SD, minimum, and maximum, all measured in millimeters. These metrics provide a comprehensive evaluation of the models' performance in estimating the properties of the wood cross-sectional images.

The validation datasets consisted of Parawood cross-sectional images and Douglas Fir cross-sectional images. The Parawood dataset contained 900 images, while the Douglas Fir dataset comprised 65 images. By including the Douglas Fir dataset, we aimed to assess the generalizability and robustness of our models across different wood species.

In the following section, we will present the experimental results, including the performance of the models trained using different architectures, optimizers, regression functions, and numbers of epochs. This analysis will provide insights into the effectiveness and suitability of our proposed approach for pith estimation in wood cross-sectional datasets.

#### 3.1. Parawood Cross-sectional Dataset

Figure 2-a displays the boxplot representing the distribution of mean errors in pith estimation for the Parawood cross-sectional dataset. Only configurations of the model that yielded a mean error of less than 100 are included in the plot. The central horizontal lines in each boxplot indicate the mean errors, providing a summary of the average performance of the models. Notably, Xception emerges as the top-performing model among the three architectures, exhibiting a lower mean error compared to ResNet50 and MobileNet.

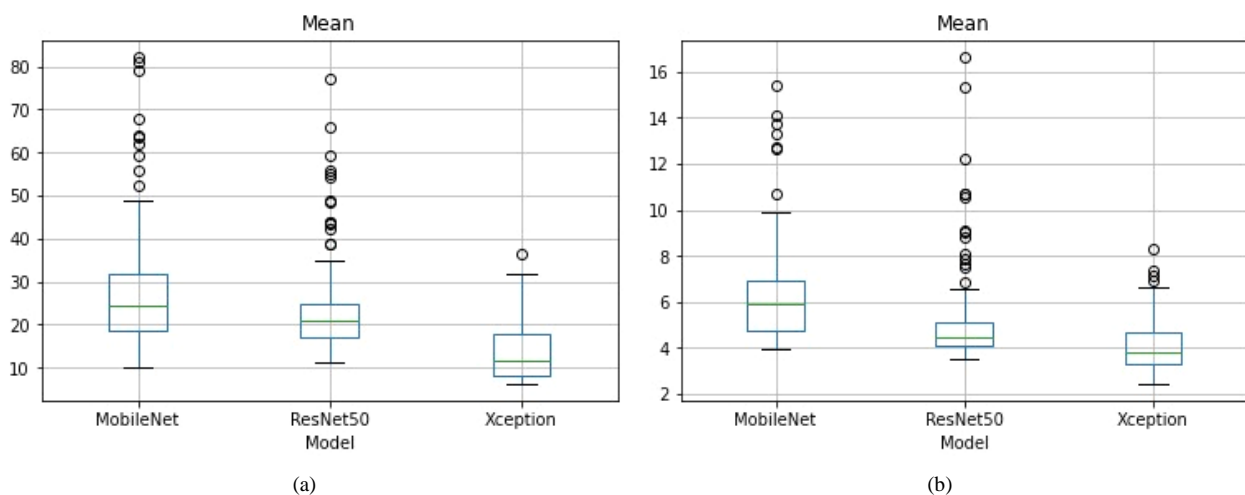
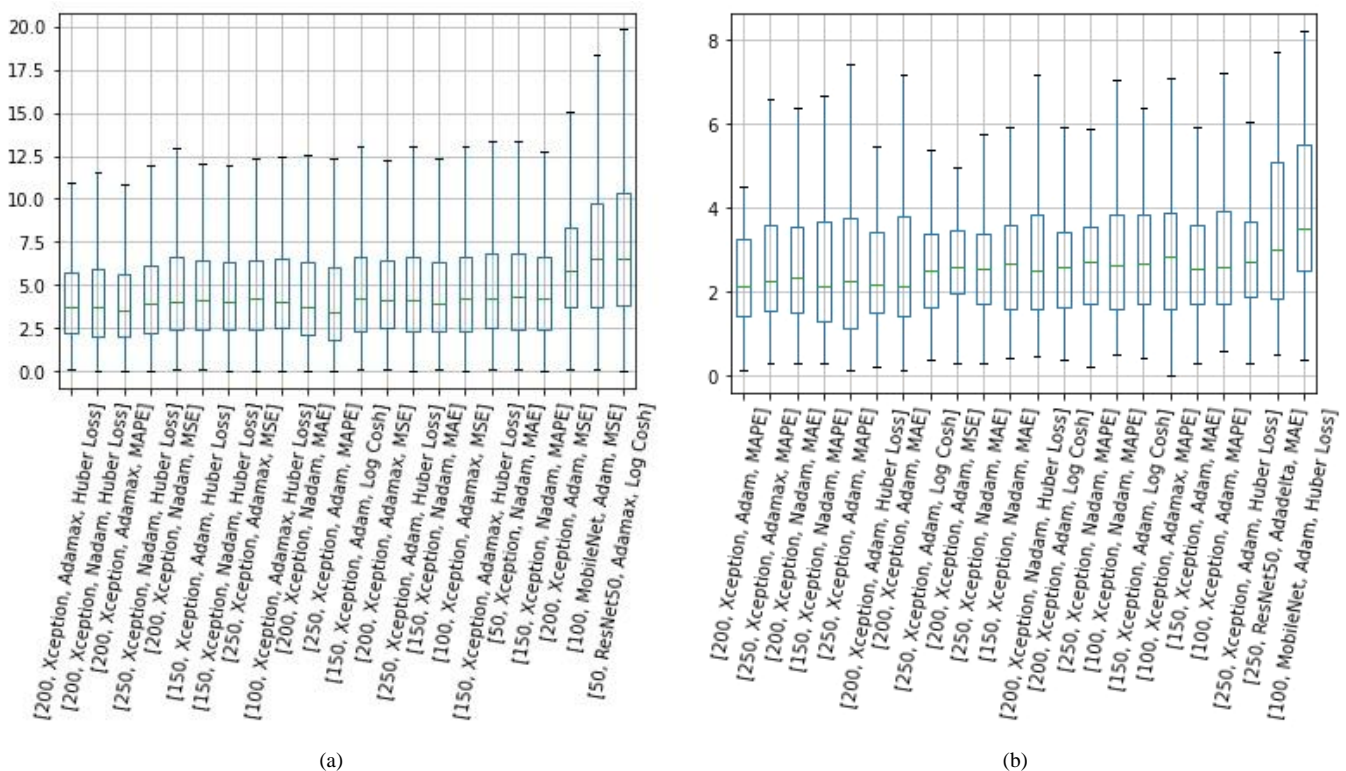


Figure 2. Comparison of mean errors: boxplot illustrating the distribution of mean errors for the top 20 performing models and the first occurrences of MobileNet and ResNet50 on the Parawood cross-sectional dataset

The boxplot in Figure 3-a provides a visual representation of the distribution of mean errors for the top 20 performing models and the first occurrences of other models (MobileNet and ResNet50) on the Parawood cross-sectional dataset. The vertical axis of the boxplot represents the mean errors in millimeters, while the horizontal axis represents the different models.



**Figure 3. Comparison of mean errors: boxplot illustrating the distribution of mean errors for the top 20 performing models and the first occurrences of ResNet50 and MobileNet on the Douglas Fir cross-sectional datasets**

Upon analyzing the boxplot, several key findings emerge. Firstly, it is evident that the top 20 performing models are primarily based on the Xception architecture. This observation suggests that the Xception model consistently outperforms MobileNet and ResNet50 in terms of mean error estimation on the Parawood cross-sectional dataset. Furthermore, all the models, including the top 20 performing models and the first occurrences of MobileNet and ResNet50, exhibit a narrow interquartile range (IQR). The IQR, represented by the length of the box in the boxplot, provides a measure of the spread or variability of the mean errors within each group of models. The narrow IQR across all models indicates that the errors are tightly concentrated around the median, reflecting a relatively consistent and precise performance.

These findings collectively reinforce the superiority of the Xception models among the top-performing models. The consistently lower mean errors and the narrow IQR demonstrate the superior performance and accuracy of the Xception architecture in estimating the pith location on the Parawood cross-sectional dataset.

In accordance with the boxplot results, Table 2 provides a comprehensive overview of the top 20 models evaluated on the Parawood cross-sectional dataset, including the first occurrences of MobileNet and ResNet50. The consistent findings highlight the superior performance of models trained with the Xception architecture in accurately estimating the properties of the Parawood cross-sectional dataset. Among the top-performing models, the Xception model trained with the Adam optimizer and the Huber Loss regression function achieved the lowest mean absolute percentage error of 4.45 millimeters. The performance of the models ranged from a minimum mean absolute percentage error of 0.07 millimeters to a maximum of 46.66 millimeters. These results underscore the effectiveness of the Xception model in accurately estimating the pith location in the Parawood cross-sectional dataset.

**Table 2. Top 20 performing models on the Parawood cross-sectional dataset**

Epoch	Model	Optimizer	Regression Function	Mean	SD	Min	Max	Note	
1	200	Xception	Adamax	Huber Loss	4.45	3.71	0.07	46.66	
<b>2</b>	<b>200</b>	<b>Xception</b>	<b>Nadam</b>	<b>Huber Loss</b>	<b>4.48</b>	<b>3.69</b>	<b>0.00</b>	<b>40.75</b>	Common
3	200	Xception	Adamax	MAPE	4.53	4.22	0.00	44.70	
4	250	Xception	Nadam	Huber Loss	4.72	3.82	0.00	39.60	
5	200	Xception	Nadam	MSE	4.90	3.64	0.07	25.73	
6	150	Xception	Adam	Huber Loss	4.93	4.10	0.07	53.38	
7	150	Xception	Nadam	Huber Loss	4.93	4.24	0.00	52.79	
8	250	Xception	Adamax	MSE	4.99	4.32	0.00	48.68	
9	100	Xception	Adamax	Huber Loss	5.02	4.10	0.00	39.79	
10	200	Xception	Nadam	MAE	5.04	4.88	0.00	45.97	
11	250	Xception	Adam	MAPE	5.04	5.68	0.00	46.07	
12	150	Xception	Adam	Log Cosh	5.06	4.08	0.07	38.21	
13	200	Xception	Adamax	MSE	5.07	4.31	0.10	36.66	
14	250	Xception	Adam	Huber Loss	5.08	4.32	0.00	51.73	
15	150	Xception	Nadam	MAE	5.11	4.90	0.07	58.86	
16	100	Xception	Adamax	MSE	5.11	4.33	0.00	44.14	
17	150	Xception	Adamax	Huber Loss	5.13	4.12	0.07	43.40	
18	50	Xception	Nadam	MAE	5.15	4.35	0.07	47.50	
19	150	Xception	Nadam	MAPE	5.18	4.80	0.00	66.59	
20	100	Xception	Adamax	MAPE	5.19	4.27	0.00	46.13	
:	:	:	:	:	:	:	:		
70	100	MobileNet	Adam	MSE	7.32	5.10	0.15	41.68	
:	:	:	:	:	:	:	:		
82	50	ResNet50	Adamax	Log Cosh	7.94	6.10	0	49.49	

Notably, it is worth mentioning that the first occurrence of MobileNet trained with 100 epochs using the Adam optimizer and the MSE regression function is observed at index 70. This model demonstrated the following statistics: a mean of 7.32 millimeters, a standard deviation of 5.10 millimeters, a minimum of 0.15 millimeters, and a maximum of 41.68 millimeters. Comparatively, the mean of this model is approximately 1.6 times higher than that of the first model in the table.

Similarly, the first occurrence of ResNet50 trained with 50 epochs using the Adamax optimizer and the Log Cosh regression function is observed at index 82. This model displayed the following statistics: mean of 7.94 millimeters, standard deviation of 6.10 millimeters, minimum of 0 millimeters, and maximum of 49.49 millimeters. These statistics indicate that this model has a mean approximately 1.6 times higher than the first model in the table.

These additional instances highlight the variability in model performance based on different combinations of architectures, optimizers, regression functions, and numbers of epochs. Despite not being included in the top 20 models, these occurrences provide further insights into the range of performance observed in the Parawood cross-sectional dataset.

### 3.2. Douglas Fir Cross-sectional Dataset

Figure 2-b displays a boxplot representing the distribution of mean errors in pith estimation for the Douglas Fir cross-sectional dataset. The boxplot focuses on configurations of the model that resulted in a mean error of less than 100. The central horizontal lines within each boxplot indicate the mean errors, providing an overview of the average performance of the models. Notably, the Xception architecture emerges as the top-performing model among the three architectures, exhibiting a lower mean error compared to ResNet50 and MobileNet. This highlights the superior performance and accuracy of the Xception model in estimating the properties of the Douglas Fir cross-sectional dataset.

Similarly, the boxplot in Figure 3-b presents the distribution of mean errors for the top 20 performing models and the first occurrences of ResNet50 and MobileNet on the Douglas Fir dataset. Upon analyzing the boxplot, we observe similar tendencies to those observed in the Parawood cross-sectional dataset. Once again, the top 20 performing models predominantly belong to the Xception architecture, indicating its consistent superiority over ResNet50 and MobileNet in terms of mean error estimation on the Douglas Fir cross-sectional dataset.

Additionally, all the models, including the top 20 performing models and the first occurrences of ResNet50 and MobileNet, demonstrate a narrow IQR in their distribution of mean errors. The narrow IQR observed in these models indicates a high degree of precision and consistency in their performance, as the majority of the mean errors fall within a relatively small range. This reinforces the reliability and consistency of these models, further highlighting their effectiveness in accurately estimating the pith location.

These findings reaffirm the effectiveness of the Xception models in accurately estimating the pith location on the Douglas Fir cross-sectional dataset. The consistently lower mean errors and the narrow IQR further support the superior performance of the Xception architecture compared to ResNet50 and MobileNet.

Table 3 presents the results of the top 20 models evaluated on the Douglas Fir cross-sectional dataset, including the first occurrences of MobileNet and ResNet50. Similar to the experiments conducted on the Parawood cross-sectional dataset, the ResNet50, MobileNet, and Xception architectures were trained with various optimizers, regression functions, and numbers of epochs. The evaluation metrics used include mean, SD, minimum, and maximum, all measured in millimeters. These metrics provide a comprehensive assessment of the model performance in pith estimation for the Douglas Fir cross-sectional dataset.

**Table 3. Top 20 performing models on the Douglas Fir cross-sectional dataset**

	Epoch	Model	Optimizer	Regression Function	Mean	SD	Min	Max	Note
1	200	Xception	Adam	MAPE	2.43	1.35	0.14	6.48	
2	250	Xception	Adamax	MAPE	2.59	1.51	0.32	6.67	
3	200	Xception	Nadam	MAE	2.59	1.48	0.32	7.01	
4	150	Xception	Nadam	MAPE	2.62	1.67	0.28	7.63	
5	250	Xception	Adam	MAPE	2.63	1.76	0.14	7.43	
6	200	Xception	Adam	Huber Loss	2.63	1.67	0.20	10.01	
7	200	Xception	Adam	MAE	2.68	1.75	0.14	7.20	
8	250	Xception	Adam	Log Cosh	2.71	1.46	0.40	6.98	
9	200	Xception	Adam	MAE	2.74	1.29	0.28	6.55	
10	250	Xception	Nadam	MAE	2.75	1.64	0.32	9.06	
11	150	Xception	Nadam	MAE	2.81	1.53	0.42	7.60	
<b>12</b>	<b>200</b>	<b>Xception</b>	<b>Nadam</b>	<b>Huber Loss</b>	<b>2.81</b>	<b>1.57</b>	<b>0.45</b>	<b>7.18</b>	Common
13	200	Xception	Adam	Log Cosh	2.85	1.58	0.40	7.79	
14	250	Xception	Nadam	MAPE	2.85	1.60	0.20	8.27	
15	100	Xception	Nadam	MAPE	2.93	1.71	0.51	7.23	
16	150	Xception	Adam	Log Cosh	2.95	1.74	0.42	8.89	
17	100	Xception	Adamax	MAPE	2.96	1.62	0.00	7.09	
18	150	Xception	Adam	MAE	2.97	1.76	0.28	9.29	
19	100	Xception	Adam	MAPE	2.97	1.57	0.58	7.70	
20	250	Xception	Adam	Huber Loss	2.97	1.62	0.28	8.30	
:	:	:	:	:	:	:	:		
58	250	ResNet50	Adadelata	MAE	3.50	1.96	0.51	7.73	
:	:	:	:	:	:	:	:		
115	100	MobileNet	Adam	Huber Loss	3.93	2.20	0.40	11.83	

Among the evaluated models, those based on the Xception architecture demonstrated superior performance in accurately estimating the properties of the Douglas Fir cross-sectional dataset. Specifically, the model trained with Xception using the Adam optimizer and the MAPE regression function achieved the lowest mean error of 2.43 millimeters. The performance of the models ranged from a minimum mean error of 0.14 millimeters to a maximum of 6.48 millimeters.

Furthermore, it is noteworthy that the first occurrence of ResNet50 with the Adadelta optimizer and the MAE regression function is at index 58, achieving a mean error of 3.50 millimeters, with a standard deviation of 1.96 millimeters, a minimum of 0.51 millimeters, and a maximum of 7.73 millimeters. Similarly, the first occurrence of MobileNet with the Adam optimizer and the Huber Loss regression function is at index 115, achieving a mean error of 3.93 millimeters, with a standard deviation of 2.20 millimeters, a minimum of 0.40 millimeters, and a maximum of 11.83 millimeters. These models exhibit approximately 1.5 times the mean error compared to the top-performing model.

These results highlight the effectiveness of the Xception architecture in estimating the properties of the Douglas Fir cross-sectional dataset. However, it is important to acknowledge that the performance of the models can vary depending on the chosen architecture, optimizer, regression function, and number of epochs. Further analysis and experimentation are necessary to determine the optimal configuration for different wood species and datasets.

### 3.3. Comparison and Analysis

Upon meticulous examination of the results from both datasets, we observed an intriguing trend: the top-performing models on the Parawood cross-sectional dataset consistently demonstrated competitive performance on the Douglas Fir cross-sectional dataset. This observation highlights the robustness and generalizability of our models across different wood species. Nevertheless, we must exercise caution in interpreting these results, as variations in pith estimation performance between datasets were evident. These variations likely stem from inherent differences in wood characteristics, such as grain patterns, texture, and color, along with diverse imaging conditions, including lighting and camera angles.

Of particular note is the Xception model, which emerged as the common winner. This model showcased remarkable consistency and promise on both the Parawood and Douglas Fir cross-sectional datasets. Specifically, the model configuration that achieved the status of 'common winner' involved training the Xception architecture with 200 epochs, employing the Nadam optimizer, and implementing the Huber Loss regression function (for more detailed information, please refer to the rows marked 'Common' in Tables 2 and 3).

On the Parawood cross-sectional dataset, our common winner model exhibited a mean error of 4.48 millimeters, accompanied by a standard deviation of 3.69 millimeters. These figures underline the impressive accuracy and reliability of this model in estimating the pith location within the Parawood cross-sectional dataset.

Similarly, on the Douglas Fir cross-sectional dataset, the common winner achieved a mean error of 2.81 millimeters, complemented by a standard deviation of 1.57 millimeters. These results reinforce the model's efficacy and dependability in estimating the pith location within the Douglas Fir cross-sectional dataset. The consistency in the model's performance across these datasets underscores the effectiveness and generalizability of the Xception model for estimating the pith location, irrespective of the wood species under consideration. Notably, this model consistently outperformed its ResNet50 and MobileNet counterparts across both datasets.

Further dissection of the results reveals the influence of various factors. Specifically, the choice of optimization algorithm, regression function, and training duration significantly impacted the model's performance. Among the array of configurations tested, the combination of the Adamax optimizer and the Huber Loss regression function consistently stood out, yielding models with notably low mean errors and standard deviations. This attests to the pivotal role played by these elements in accurate pith estimation and highlights their suitability for regression-based tasks in this context.

To provide a comprehensive visual assessment of our model's accuracy in estimating pith locations within the Parawood cross-sectional dataset, we present a series of images in Figure 4. In each image, the ground truth pith location is indicated by a white plus sign, while the estimated pith location derived from our model, trained over 200 epochs with the Xception architecture, Adamax optimizer, and Huber Loss regression function, is marked by blue cross signs. Furthermore, the precise error distance between the ground truth and the estimated pith location is displayed in the top left corner of each image. These images offer a vivid and informative illustration of our model's capabilities in accurately determining pith locations within the Parawood cross-sectional dataset.

In addition to presenting the overall pith estimation results, we identified a subset of outliers within the Parawood cross-sectional dataset, comprising approximately 4.67% of the total dataset. This subset encompasses 42 images characterized by pith estimation errors exceeding 11 millimeters. Figure 5 showcases these specific images, shedding light on the challenging cases where our model encountered difficulty in accurately estimating pith locations. Importantly, the estimations presented in these images were generated using the Xception model, trained over 200 epochs, utilizing the Adamax optimizer, and implementing the Huber Loss regression function. A comprehensive analysis of these outliers allows us to glean profound insights into the limitations and potential areas for enhancement in our pith estimation approach.



Figure 4. Pith estimation results for Parawood cross-sectional dataset: comparison of ground truth and model predictions



Figure 5. Outliers of pith estimation in Parawood cross-sectional dataset

In summation, our meticulously designed experiments validate the robustness and reliability of the Xception model, particularly when trained with our selected parameters, for pith estimation within wood cross-sectional datasets. The model's consistent performance across both the Parawood and Douglas Fir datasets accentuates its effectiveness and adaptability across diverse wood species. In our forthcoming analysis, we will undertake a rigorous comparison of the

performance of the common winner model with the benchmarked results from Kurdthongmee et al. [17] and Decelle et al. [22]. This comparative analysis promises to provide invaluable insights into the competitiveness and the extent of advancements achieved by our proposed approach.

### 3.4. Benchmarking Results

In this subsection, we compare the performance of our common winner model with the benchmarked results from Kurdthongmee et al. [17] and Decelle et al. [22] on the Parawood and Douglas Fir cross-sectional datasets, respectively. We first provide a summary of the approaches used by these benchmarked studies. Kurdthongmee et al. proposed a method for pith detection in cross-sectional images of Parawood using deep neural network object detection algorithms [17]. They specifically applied the SSD MobileNet object detection algorithm and achieved a detection rate of 87.7%. Their approach involved training the model on a dataset consisting of Parawood cross-sectional images and utilizing the mean error as the evaluation metric. Decelle et al. presented an alternative approach for estimating the pith position on images of Douglas Fir tree log ends using ant colony optimization [22]. Their method focused on optimizing the detection algorithm by iteratively adjusting the parameters and evaluating the fitness of the ant colony optimization algorithm. The performance of their approach was evaluated using statistical measures such as mean, SD, minimum, maximum, and processing time (in milliseconds).

Now, we proceed to compare the performance of our common winner model with the benchmarked results from Kurdthongmee et al. [17] and Decelle et al. [22] providing insights into the effectiveness and competitiveness of our approach. The benchmarking results of pith detection on the Parawood cross-sectional dataset were compared between our common winner model, Xception with an epoch of 200, Adamax optimizer, and Huber Loss regression function, and the approach proposed by Kurdthongmee et al. [17]. Table 4 provides a summary of the performance metrics, including the detection rate, SD, minimum, maximum, and time (in milliseconds), for both approaches.

**Table 4. Comparison of pith detection performance - common winner vs. Kurdthongmee et al. [17] on the Parawood cross-sectional dataset**

Approach	Detection Rate	Mean	SD	Min	Max	Time
Common Winner	100	4.48	3.69	0.00	40.75	505
Kurdthongmee et al. [17]	87.7	7.04	15.32	0.11	193.19	780

Our common winner models demonstrated exceptional performance on the Parawood cross-sectional dataset. They achieved a detection rate of 100%, successfully estimating the pith in all images. The better-performing winner model exhibited a low mean error of 4.48, highlighting its accuracy in estimating the pith location. Furthermore, the model displayed consistency in its estimations, as indicated by the low standard deviation of 3.69. The range of estimation errors spanned from a minimum of 0.00 to a maximum of 40.75, showcasing the model's ability to capture the full spectrum of estimation accuracy. Moreover, our model showcased remarkable efficiency, with an average processing time per image recorded as 505 milliseconds, which is approximately 65% of the processing time taken by the benchmarked approach. These results demonstrate the effectiveness of our model in accurately estimating the pith while maintaining fast processing times.

In comparison, the benchmarked approach of Kurdthongmee et al. [17] achieved a detection rate of 87.7% on the Parawood cross-sectional dataset, with a mean error of 7.04. The standard deviation of 15.32 indicated a larger variation in the estimation errors compared to our common winner model. The range of errors spanned from a minimum of 0.11 to a maximum of 193.19. Additionally, the average processing time per image was reported as 780 milliseconds.

These results clearly demonstrate that our common winner model outperforms the benchmarked approach of Kurdthongmee et al. [17] across all evaluation metrics on the Parawood cross-sectional dataset. Our model achieved higher accuracy with a lower mean error, a narrower range of estimation errors, and a faster processing time per image. This validates the effectiveness and competitiveness of our approach in pith estimation on the Parawood cross-sectional dataset. The pith estimation results on the Douglas Fir cross-sectional dataset were compared between our common winner model and the approach proposed by Decelle et al. [22]. Table 5 presents a comprehensive overview of the performance metrics for both approaches, including mean, SD, minimum, and maximum values.

The results from Table 5 demonstrate that our common winner models achieved slightly higher mean values compared to the approach by Decelle et al. [22]. However, the SD, minimum, and maximum values indicate a similar range of pith estimation accuracy between the two approaches. Notably, our common winner models outperformed the benchmarked approach in terms of average processing time per image, requiring only half the time to estimate the pith. This showcases the efficiency of our model without compromising on the accuracy of pith estimation.

**Table 5. Benchmarking results: common winner vs. Decelle et al. [22] on Douglas Fir cross-sectional dataset**

Approach	Mean	SD	Min	Max	Time
Common Winner	2.81	1.57	0.45	7.18	505
Decelle et al. [22]	2.26	1.32	0.44	4.63	1,055

### 3.5. Analysis of Optimizers and Regression Functions for Pith Estimation

In this subsection, we explore various combinations of optimizers and regression functions that yield acceptable mean error for pith estimation. Table 6 showcases the frequency counts for each optimizer-regression function combination. To obtain these results, we examined all models and checked whether their mean error was below 7.5. If so, we recorded the corresponding regression function and optimizer used during training, updating the frequency count for that specific combination. For example, the combination of Adadelta optimizer and MAPE regression function resulted in 10 models with a mean error less than 7.5.

**Table 6. Frequency analysis of optimizers and regression functions for pith estimation**

Regression Functions	Optimizers						
	Adam	Adagrad	Adadelta	Nadam	Adamax	RMSprop	SGD
MSE	4	5	4	3	5	1	0
MAE	4	4	4	5	5	0	0
Log Cosh	0	0	0	1	0	0	0
Huber Loss	5	4	4	5	5	1	0
MAPE	9	9	10	9	10	5	0
MSLE	1	0	0	0	2	2	0
Cosine Similarity	0	0	0	0	0	0	0

From the table, we can infer that the SGD optimizer performed poorly when used to train the models, as it produced none of the models with an acceptable mean error, regardless of the regression function employed. Similarly, the Cosine Similarity regression function did not yield any models with an acceptable mean error, despite using various optimizers. These findings suggest that, for this specific regression problem, training models using Log Cosh, MSLE, or Cosine Similarity regression functions may not be effective. Additionally, training models using the SGD optimizer may not be fruitful.

The frequency analysis of optimizers and regression functions provides valuable insights into the modeling choices and preferences in pith estimation. It offers a glimpse into the strategies employed by the models to achieve accurate estimation results. Future research could delve deeper into the impact of different optimizer-regression function combinations on model performance and explore alternative combinations to potentially enhance estimation accuracy.

### 3.6. Discussions

The results of our experiments demonstrate the effectiveness of our proposed approach for pith estimation in both the Parawood and Douglas Fir cross-sectional datasets. The top 20 performing models achieved competitive mean errors ranging from 4.45 to 5.18 for the Parawood cross-sectional dataset and from 2.43 to 2.97 for the Douglas Fir cross-sectional dataset, affirming the accuracy of our approach in estimating pith locations in different wood species.

The selection of ResNet50, MobileNet, and Xception as the base models for feature extraction proved beneficial, with all three architectures consistently yielding top-performing models. Among them, Xception particularly stood out, underscoring its effectiveness for this specific task.

The choice of optimizers, regression functions, and the number of epochs significantly influenced the model performance. The combination of the Adamax optimizer and the Huber Loss regression function consistently produced top-performing models with relatively low mean errors and standard deviations. Importantly, the analysis of various epoch settings revealed that simply increasing the number of epochs does not guarantee improved performance, highlighting the importance of selecting appropriate optimization algorithms, loss functions, and epoch counts for regression-based tasks. When comparing the results between the Parawood and Douglas Fir cross-sectional datasets, we observed similar trends in model performance, indicating the robustness and generalizability of our approach. The top-performing models achieved competitive results on both datasets, further illustrating the versatility and effectiveness of our approach.

Furthermore, our common winning model demonstrated faster processing times compared to the benchmarked models on both the Parawood and Douglas Fir cross-sectional datasets. With an average processing time per image of 505 milliseconds, our model was approximately 65% faster than the benchmarked approach on the Parawood cross-sectional dataset. Similarly, on the Douglas Fir cross-sectional dataset, our model exhibited superior efficiency, taking only half the time to estimate pith locations compared to the benchmarked approach. This notable reduction in processing times emphasizes the efficiency and computational advantage of our proposed approach.

In this research, the theoretical approach is founded on the principles of deep learning and computer vision. We employ convolutional neural networks (CNNs) as the backbone of our approach, specifically ResNet50, MobileNet, and Xception, which are renowned architectures in the field. These CNNs are chosen for their capacity to extract intricate features from images, making them well-suited for the task of pith estimation in wood cross-sectional images.

The theoretical foundation of our approach revolves around adapting these CNNs for regression-based tasks. Unlike conventional approaches that employ these architectures for classification purposes, we fine-tune their architecture and objectives to make them adept at predicting the precise location of the pith in wood samples. This shift from classification to regression forms the crux of our theoretical approach, enabling us to achieve highly accurate and consistent pith estimations.

Moreover, our theoretical framework encompasses the critical aspect of optimization. We delve into the selection of optimizers and regression functions, recognizing their pivotal role in shaping model performance. The choice of the Adamax optimizer and the Huber Loss regression function emerged from careful consideration, as they consistently yielded models with superior performance, demonstrating the theoretical underpinning of our approach's success.

In tandem with these aspects, we also explore the impact of varying the number of training epochs. This theoretical investigation serves to elucidate the nuanced relationship between training duration and model efficacy, emphasizing the importance of thoughtful epoch selection in regression tasks.

Furthermore, our approach is theoretically grounded in its capacity to generalize across different wood species. We probe the theoretical aspects of model robustness by evaluating its performance on both Parawood and Douglas Fir datasets, confirming that the theoretical underpinnings of our approach extend to diverse wood types. Ultimately, our theoretical approach converges on enhancing the efficiency and precision of pith estimation in wood cross-sectional images through deep learning. By adapting state-of-the-art CNNs, optimizing their parameters, and rigorously testing them on diverse datasets, our research is firmly rooted in theoretical principles that underpin the development of practical, efficient, and accurate pith estimation methods for the wood products industry.

#### 4. Conclusion

In conclusion, our study presents a comprehensive analysis of pith estimation in wood cross-sectional images using deep learning techniques. We proposed an effective approach that leverages popular deep neural network architectures, including ResNet50, MobileNet, and Xception, for feature extraction. Through extensive experiments on the Parawood and Douglas Fir cross-sectional datasets, we evaluated the performance of different models trained with various optimizers, regression functions, and numbers of epochs. The results demonstrated the effectiveness of our proposed approach in accurately estimating the location of the pith in wood cross-sectional images. The top-performing models achieved competitive mean errors, indicating their accuracy in pith estimation. Among the architectures, Xception consistently performed well, showcasing its effectiveness for this specific task. The choice of optimizers and regression functions also played a crucial role in model performance, with the combination of the Adamax optimizer and the Huber Loss regression function consistently producing top-performing models. Furthermore, our approach exhibited robustness and generalizability across different wood species. The models achieved competitive results on both the Parawood and Douglas Fir cross-sectional datasets, demonstrating the versatility and effectiveness of our approach. Moreover, our common winner model showcased not only high accuracy but also superior efficiency, achieving faster processing times compared to benchmarked approaches, highlighting the efficiency and computational advantage of our proposed approach.

Looking to the future, there are several exciting avenues for further research in this domain. The standard deviations of the errors indicate potential areas for refinement, suggesting avenues for future research. Additional architectural modifications, fine-tuning of hyperparameters, and the exploration of advanced techniques such as ensemble learning could further enhance the performance of the models. Additionally, the application of our approach to other wood species and the investigation of its adaptability to varying wood quality conditions are promising directions for future research. Overall, our study not only contributes to the advancement of pith estimation techniques in the wood products industry but also points toward exciting opportunities for future research and development. By providing accurate and efficient estimations, our proposed approach has the potential to improve productivity and streamline operations in wood processing. The findings presented in this research not only address current challenges but also lay the foundation for continued exploration and innovation in automated pith estimation methods.

## 5. Declarations

### 5.1. Data Availability Statement

The data presented in this study are available on request from the corresponding author.

### 5.2. Funding

This research was financially supported by the Rubber Authority of Thailand (RAOT) under the project “The development of an automatic system to convey, align axis and saw into wood palettes for productivity enhancement of rubber wood processing”.

### 5.3. Institutional Review Board Statement

Not applicable.

### 5.4. Informed Consent Statement

Not applicable.

### 5.5. Declaration of Competing Interest

The author declares that he has no known competing financial interests or personal relationships that could have appeared to influence the work reported in this paper.

## 6. References

- [1] Islam, M. N., Rahman, F., Das, A. K., & Hiziroglu, S. (2022). An overview of different types and potential of bio-based adhesives used for wood products. *International Journal of Adhesion and Adhesives*, 112, 102992. doi:10.1016/j.ijadhadh.2021.102992.
- [2] Hakkou, M., Pétrissans, M., Zoulalian, A., & Gérardin, P. (2005). Investigation of wood wettability changes during heat treatment on the basis of chemical analysis. *Polymer Degradation and Stability*, 89(1), 1–5. doi:10.1016/j.polymdegradstab.2004.10.017.
- [3] Denih, A., Putra, G. R., Kurniawan, Z., & Bahtiar, E. T. (2023). Developing a Model for Curve-Fitting a Tree Stem’s Cross-Sectional Shape and Sapwood–Heartwood Transition in a Polar Diagram System Using Nonlinear Regression. *Forests*, 14(6), 1102. doi:10.3390/f14061102.
- [4] Hänsel, A., Sandak, J., Sandak, A., Mai, J., & Niemz, P. (2022). Selected previous findings on the factors influencing the gluing quality of solid wood products in timber construction and possible developments: A review. *Wood Material Science & Engineering*, 17(3), 230–241. doi:10.1080/17480272.2021.1925963.
- [5] Longuetaud, F., Schraml, R., Mothe, F., Ravoajanahary, T., Decelle, R., Constant, T., ... & Uhl, A. (2023). Traceability and quality assessment of Norway spruce (*Picea abies* (L.) H. Karst.) logs: the TreeTrace\_spruce database. *Annals of Forest Science*, 80(1), 9. doi:10.1186/s13595-023-01178-8.
- [6] Longuetaud, F., Pot, G., Mothe, F., Barthelemy, A., Decelle, R., Delconte, F., ... & Viguier, J. (2022). TreeTrace project database on traceability and quality assessment of round woods: Douglas fir sampling. *Annals of Forest Science*, 79(46), 1–22. doi:10.1186/s13595-022-01163-7.
- [7] Longuetaud, F., Leban, J. M., Mothe, F., Kerrien, E., & Berger, M. O. (2004). Automatic detection of pith on CT images of spruce logs. *Computers and Electronics in Agriculture*, 44(2), 107–119. doi:10.1016/j.compag.2004.03.005.
- [8] Entacher, K., Hegenbart, S., Kerschbaumer, J., Lenz, C., Planitzer, D., Seidel, M., Uhl, A., & Weiglmaier, R. (2008). Pith detection on CT-Cross-Section images of logs: An experimental comparison. 2008 3<sup>rd</sup> International Symposium on Communications, Control and Signal Processing. doi:10.1109/isccsp.2008.4537273.
- [9] Krähenbühl, A., Kerautret, B., Debled-Rennesson, I., Longuetaud, F., & Mothe, F. (2012). Knot Detection in X-Ray CT Images of Wood. *Advances in Visual Computing. ISVC 2012. Lecture Notes in Computer Science*, 7432, Springer, Berlin, Germany. doi:10.1007/978-3-642-33191-6\_21.
- [10] Boukadida, H., Longuetaud, F., Colin, F., Freyburger, C., Constant, T., Leban, J. M., & Mothe, F. (2012). PithExtract: A robust algorithm for pith detection in computer tomography images of wood – Application to 125 logs from 17 tree species. *Computers and Electronics in Agriculture*, 85, 90–98. doi:10.1016/j.compag.2012.03.012.
- [11] Kurdthongmee, W., Suwannarat, K., Panyuen, P., & Sae-Ma, N. (2018). A Fast Algorithm to Approximate the Pith Location of Rubberwood Timber from a Normal Camera Image. 2018 15<sup>th</sup> International Joint Conference on Computer Science and Software Engineering (JCSSE), Nakhonpathom, Thailand. doi:10.1109/jcsse.2018.8457375.
- [12] Kurdthongmee, W., & Suwannarat, K. (2019). An efficient algorithm to estimate the pith location on an untreated end face image of a rubberwood log taken with a normal camera. *European Journal of Wood and Wood Products*, 77(5), 919–929. doi:10.1007/s00107-019-01433-8.

- [13] Hanning, T., Kickingereder, R., & Casasent, D. (2003). Determining the average annual ring width on the front side of lumber. *Optical Measurement Systems for Industrial Inspection III*, Munich, Germany. doi:10.1117/12.500200.
- [14] Österberg, P., Ihalainen, H., & Ritala, R. (2004). Method for analyzing and classifying wood quality through local 2d-spectrum of digital log end images. *Proceedings of International Conference on Advanced Optical Diagnostics in Fluids, Solids and Combustion, VSJ-SPIE'04*, 4-6 December, 2004, Tokyo, Japan.
- [15] Norell, K., & Borgfors, G. (2008). Estimation of pith position in untreated log ends in sawmill environments. *Computers and Electronics in Agriculture*, 63(2), 155–167. doi:10.1016/j.compag.2008.02.006.
- [16] Kurdthongmee, W., & Suwannarat, K. (2019). Locating Wood Pith in a Wood Stem Cross Sectional Image Using YOLO Object Detection. *2019 International Conference on Technologies and Applications of Artificial Intelligence (TAAI)*, Kaohsiung, Taiwan. doi:10.1109/taai48200.2019.8959823.
- [17] Kurdthongmee, W. (2020). A comparative study of the effectiveness of using popular DNN object detection algorithms for pith detection in cross-sectional images of parawood. *Heliyon*, 6(2), 3480. doi:10.1016/j.heliyon.2020.e03480.
- [18] Kurdthongmee, W., Suwannarat, K., & Kiplagat, J. (2022). A Framework to Create a Deep Learning Detector from a Small Dataset: A Case of Parawood Pith Estimation. *Emerging Science Journal*, 7(1), 245–255. doi:10.28991/esj-2023-07-01-017.
- [19] He, K., Zhang, X., Ren, S., & Sun, J. (2016). Deep Residual Learning for Image Recognition. *2016 IEEE Conference on Computer Vision and Pattern Recognition (CVPR)*, Las Vegas, United States. doi:10.1109/cvpr.2016.90.
- [20] Howard, A. G., Zhu, M., Chen, B., Kalenichenko, D., Wang, W., Weyand, T., ... & Adam, H. (2017). Mobilenets: Efficient convolutional neural networks for mobile vision applications. *arXiv preprint*. doi:10.48550/arxiv.1704.04861.
- [21] Chollet, F. (2017). Xception: Deep Learning with Depthwise Separable Convolutions. *2017 IEEE Conference on Computer Vision and Pattern Recognition (CVPR)*. doi:10.1109/cvpr.2017.195.
- [22] Decelle, R., Ngo, P., Debled-Rennesson, I., Mothe, F., & Longuetaud, F. (2022). Ant Colony Optimization for Estimating Pith Position on Images of Tree Log Ends. *Image Processing on Line*, 12, 558–581. doi:10.5201/ipol.2022.338.